Mechanisms for Solids Ejection from Gas-Fluidized Beds

The bubble eruption process was studied in two- and three-dimensional (2D and 3D) beds using a high-speed video system for flow visualization. The results show the existence of four different ejection mechanisms; one occurring with single-bubble eruptions in both 2D and 3D beds, two others occurring in 2D and 3D beds with two bubbles coalescing at the bed-free surface, and the fourth occurring only in 3D beds with bubbles coalescing at the bed surface.

E. K. LEVY, H. S. CARAM, J. C. DILLE, and SERGIO EDELSTEIN

Energy Research Center
Lehigh University
Bethlehem, PA 18015

SCOPE

Particle elutriation is an extremely complex phenomenon which is not very well understood from a mechanistic viewpoint. Most of the available information consists of correlations of experimental data which give elutriation rate as a function of characteristics of the bed material and operating conditions; only a few investigators have studied elutriation from the fundamental perspective required for undertaking the development of quantitative mechanistic models.

In developing such physical models, information is needed on the rate and velocity at which solids are thrown above the bed by bubble eruptions. There is conflicting evidence in the literature concerning the mechanisms for solids ejection, some investigators claiming that it is principally bubble wake material which is ejected and others reporting that the bulge material at the bubble nose is thrown above the bed.

In the present investigation, flow visualization experiments were performed using a high-speed video system to obtain video tape records of the eruption process. Bubble eruptions of a wide variety were examined to determine if differences exist: between eruptions in two and three dimensional beds; between small, slow moving bubbles and large, fast moving bubbles; or between single bubbles and bubbles which coalesce near the bed surface. The objectives were to establish the source of the elutriated material, determine if more than one ejection mechanism occurs, and if so, establish when the various mechanisms are important.

CONCLUSIONS AND SIGNIFICANCE

Four different mechanisms of bubble eruption and particle ejection were observed during the course of this study. The most common eruption type was the bulge bursting mechanism which occurred in both two- and three-dimensional geometries. With this type of eruption, the bulge layer stretches and moves upward as the bubble approaches the free surface. After rising to a maximum height somewhat less than the bubble diameter and becoming leaner, the bulge particles fall back to the bed surface. The bubble wake shows a vortex structure and remains intact, gradually rising to a height of about one half that attained by the bulge before settling back onto the surface of the bed.

With a pair of three-dimensional bubbles coalescing just below the free surface, a series of events occurs. The bulge material for the leading bubble is thrown above the bed. As a result of the coalescence of the two bubbles, the layer of solids between the bubbles combines with the leading bulge layer; the resulting particle cloud expands upward and outward, and falls back to the bed surface. As the eruption process continues, the wake from the trailing bubble forms a spike which is projected above the bed surface reaching a height in excess of the height reached by the bulge and middle layers. In the case of a two-dimensional bubble eruption with coalescing bubbles, the bulge and middle layer materials erupt as in the three-dimensional case; however, the wake of the trailing bubble usually does not form a wake spike as it does in the three-dimensional case. A fourth ejection mechanism, referred to as a jet spray, was also found to occur only when two or more bubbles coalesced. In this case, a flow passage develops between the two bubbles, allowing a jet of gas to form which entrains particles and carries them to relatively large distances above the bed surface.

Of the four mechanisms, only the bulge burst, mid-layer burst and wake spike occurred often enough during the experiments to be considered important. A total of 4,228 bubbles was observed in the three-dimensional bed. Of these, 9.2% was double bubbles (two bubbles coalescing at the free surface); 3.8% of the double bubbles showed a significant jet spray, while 72.1% of the double bubbles showed a significant wake spike. Of the 1,545 bubble events observed in the two-dimensional bed, 11.3% were double bubbles, 6.9% of the double bubbles showed significant jet spray, and only 8% of the double bubbles showed significant wake spikes. The wake spikes observed in the two-dimensional apparatus, all occurred with relatively small bubbles, which were probably not truly two dimensional in character.

The experiments described above were performed with a variety of bed materials, and the results on eruption mechanisms appear to be independent of type of particle.

The results of this study help to explain why the various eruption data reported in the literature are in conflict with each other and show very clearly that research on bubble eruption behavior and particle motion in the freeboard should be carried out only in three-dimensional beds. The results reported here should be useful for future efforts on elutriation and provide a basis for beginning the development of a quantitative understanding of the relationships between the bubbling characteristics of the bed and the rate and velocities at which solids are thrown above the bed.

0001-1541-83-5733-0383-$2.00.

PREVIOUS WORK

In a series of experiments designed to test whether ejected particles originate at the nose or wake of bubbles, George and Grace (1978) dispersed very thin layers of coke particles on top of a 1-m-deep bed of sand and collected the ejected particles with a catching device located 3 cm above the bed surface. They found that the fraction of coke particles collected was always less than 4% by volume of the total; they interpreted this to mean that the vast majority of ejected particles do not originate from the surface layers but instead come from the wake. In additional experiments in which the bed was well mixed prior to ejection of bubbles, they measured the volume of ejected particles relative to bubble volume and found this to increase with bubble size. They also reported that as the bubble size increased, the material ejected with the bubbles approached the wake fraction in magnitude.

Do et al. (1972) performed experiments with glass beads of a narrow size distribution in a two-dimensional bed and obtained high-speed movies of single large bubbles and series of bubbles. Their movies showed that the ejected particles originated in the bulge material at the nose of the bursting bubbles and not from the bubble wakes.

Rowe (1965) obtained photographs which show material from the bottom of the bed reaching the bed surface during a bubble eruption; these have been interpreted widely to mean that it is wake material which is ejected.

In theoretical studies, Leva and Wen (1971) developed an analytical model which assumes that it is principally the solids carried in the bubble wake which are elutriated. Assuming spherical bubbles and using correlations for bubble size as a function of distance above the grid and for wake fraction as a function of particle characteristics, they obtained results which predict that the elutriation rates are generally several orders of magnitude less than the rate at which solids are carried up by the bubble wake. Chen and Saxena (1978), developed a theoretical model in which they assumed the solids contained in the leading bulge burst out as the bubble erupts; based on this model, they obtained a theoretical expression for solids projection rate at the bed surface.

There have also been studies dealing with particle and gas motion in the freeboard region. Zenz and Weil (1958) assumed that particles are ejected from the bed surface at a velocity of the magnitude of the bubble velocity, as it erupts into a cocurrent stream of gas rising uniformly at a rate equal to its superficial velocity through the bed. Each particle is then acted upon by inertia, gravity and drag forces; the authors performed a theoretical trajectory analysis of the particles to determine which are carried back to the bed and elutriated. They also hypothesized that the erupting bubble imposes an irregular transient jetlike velocity profile across the containing vessel and assumed that the jet velocities are eventually dissipated to the superficial gas velocity at the transport disengaging height.

Do et al. (1972), developed a trajectory analysis similar to that of Zenz and Weil and using the average superficial gas velocity in the freeboard region, computed particle trajectories from their experiments in two dimensional beds. George and Grace (1978) also used a similar trajectory analysis to deduce initial particle velocities from their elutriation data. In this case, they developed approximations for the gas jet velocities based on turbulent jet theory. Horio et al. (1980), used a hot wire anemometer probe to measure gas velocity and intensity of turbulence in the freeboard. Their results show that the bubble eruptions induce turbulent fluctuations in the gas flow and the turbulence intensity increases with erupting bubble size and decreases with bed height. Using fiber optic probe techniques to measure particle velocities and concentrations above the bed, they concluded that particle transport through the freeboard is mainly controlled by the gas velocity fluctuations induced by bubble eruptions.

APPARATUS, INSTRUMENTATION AND EXPERIMENTAL TECHNIQUE

Two fluidized beds were used for the study. The two-dimensional bed had internal cross sectional dimensions of 14.4 mm × 610 mm; the total height above the distributor was 2.44 m. The distributor was constructed from two 6.35-mm layers of ultrahigh molecular weight polyethylene sheet with a 20-micron pore size. The side walls of the bed were plexiglass.

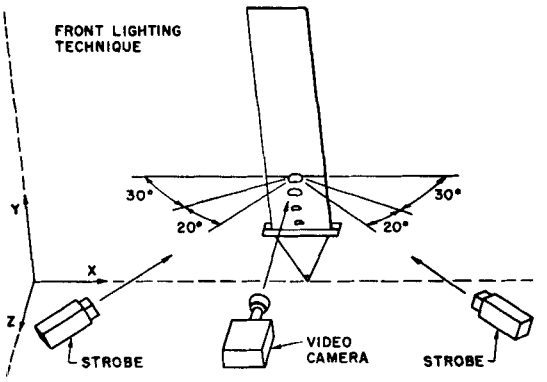

Figure 1. Front lighting technique.

The three-dimensional bed was semicircular in cross section with an inside radius of 144 mm and a height of 1.5 m. The entire bed was constructed of plexiglass except for the front face which was glass and the distributor which was made from porous stainless-steel plate with a pore size of 100 micron. The semicylindrical geometry was chosen to allow hemispherical bubbles to flow along the front planar wall within view of the camera. These more closely resemble the nearly spherical bubbles which are present in large industrial fluidized systems.

Both beds were fluidized with room temperature air at 1 atm, supplied by laboratory compressors and passed through a rotameter bank and humidification tank.

Experiments were performed in two modes of operation. In the first, bubbles of controlled size were injected into the beds which were fluidized slightly above minimum fluidization. The air for the injected bubbles was controlled by a digital timer and solenoid valve arrangement. In the second mode of operation, the beds were allowed to bubble freely at various excess air rates.

In the experiments with controlled bubble injection, the bubbles were introduced into the bed through openings in the vertical walls of the beds. In the two-dimensional case, the injection port was flush with the front face of the bed, just above the distributor. In the three-dimensional bed, the port was flush with the distributor and centered along the front face. Both ports were covered with a fine screen to prevent back flow of particles when air was not being injected. The digital timer consisted of an electronic timer and solenoid valve arrangement designed to generate from one to one thousand consecutive bubbles of controlled size. The timer could be turned off and on with pulses ranging from 0.02 to 16.6 second(s) duration, separated by adjustable intervals.

All measurements of bubble characteristics were made using a Videologic Instar high-speed video system. This device records at a rate of 120 frames per second and has slow motion replay with frame sequencing which allows each frame to be viewed separately. The camera is equipped with close-up lenses, allowing clear focusing at any distance greater than 150 mm, and two synchronized strobe lights to improve slow-motion picture quality. A schematic of the front lighting setup used in most cases is shown in Figure 1. For particles smaller than 200 μm, a thin layer of particles adhered to the walls, necessitating backlighting in the two-dimensional experiments. This technique did not give as sharp a picture as the front lighting methods, but it was still satisfactory.

In the experiments with the semicylindrical bed, it was important to know how the bubbles were truncated by the front wall. Video sequences were taken from directly above the bed pointing downward, and these showed that most of the bubbles were cut in half by the glass face.

Altogether, four different bed materials were used, Table 1. The glass beads had very narrow-size distributions with mean sizes of

TABLE 1. CHARACTERISTICS OF BED MATERIALS

Type of Material	ρ_s (kg/m^3)	$\bar{d}_p$ (μm)	U_{mf} (m/s)	ϵ_{mf}
Glass	2,450	451	0.171	0.4
Glass	2,450	125	0.0127	0.4
Styrene	1,055	765	0.08	0.38
Catalyst	3,970	112	0.01	—

TABLE 2. SIZE DISTRIBUTIONS OF STYRENE BEADS AND CATALYST

Styrene d_{pi} (μm)	wt. fraction
350–425	0.039
425–500	0.044
500–600	0.119
600–710	0.144
710–1,000	0.385
1,000–1,400	0.270
Catalyst	
50–90	0.207
90–106	0.160
106–125	0.323
125–150	0.067
150–212	0.090
212–250	0.019
250–300	0.132

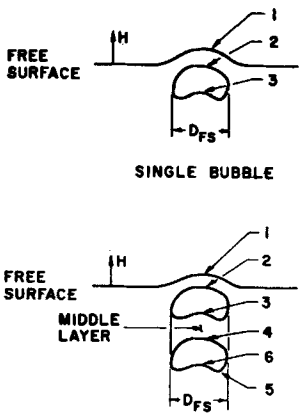

Figure 2. Bubble measurement points.

451 and 125 μm. The size distributions of the styrene beads and catalyst are shown in Table 2.

A packed-bed height between 0.49 and 0.55 m was used for most of the experiments. This depth allowed the injected bubbles to stabilize before reaching the free surface and allowed a reasonable amount of coalescence in the freely bubbling experiments. Settled depths of 0.26 and 1.04 m were also used in a few experiments to determine the influence of bed depth on frequency of the different eruption mechanisms.

Bubble velocity is a strong function of bubble size. The bubble diameter at the free surface (D_{FS}) as defined in Figure 2 ranged from 20 to 95 mm in the three-dimensional bed and from 20 to 170 mm in the two-dimensional bed. In the controlled injection experiments, bubble size was varied by changing the time of injection. Bubbles of all sizes were present at the bed surface in the freely bubbling experiments but only those which had the desired diameters and which were sufficiently removed from the effects of other bubbles were selected for analysis.

All of the controlled injection experiments were performed with gas velocities in the range of 1.05 U_{mf} to 1.08 U_{mf}. The velocities in the freely bubbling experiments ranged up to 3.44 U_{mf}. Attempts to reach higher gas velocities than these were unsuccessful, for the diameters of the erupting bubbles became large enough to

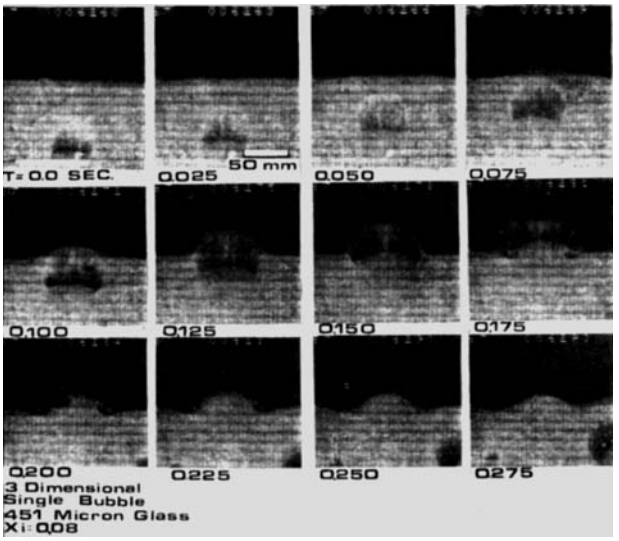

Figure 3. Three-dimensional single bubble with bulge burst.

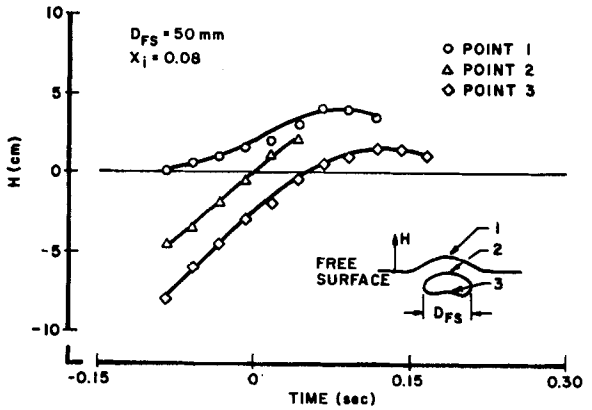

Figure 4. Trajectories of three-dimensional single bubble in 451 μm glass bed.

set up waves at the free surface which reflected from the walls of the bed and interfered with the eruption process.

Finally, it should be noted that the quantity "excess air" is defined here as $X_t \equiv U/U_{mf} - 1$.

EXPERIMENTAL RESULTS

Four different mechanisms of bubble eruption and particle ejection were observed during the course of this study. The most common eruption type is the bulge-bursting mechanism which occurred with all bed materials for all operating conditions. This is illustrated in Figure 3 for the three-dimensional case. This particular experiment was performed with 451-micron glass; the bubble was obtained by controlled injection of air, and the bubble was approximately 0.06 m in diameter at the free surface. Figure 4 is a graph of the trajectory of a similar 0.05-m three-dimensional bubble obtained with the same experimental conditions established in the previous figure. Points 1, 2 and 3 correspond to the position on the bubble centerline defined in Figure 2.

With this type of eruption, the bulge layer stretches and moves upward as the bubble approaches the free surface. After rising to a maximum height somewhat less than the bubble diameter and becoming leaner, the bulge particles (point 1) fall back to the free surface. The bubble wake (point 3) shows a vortex structure and remains intact, gradually rising to a height of about one half that attained by the bulge, before settling back onto the surface of the bed.

The two-dimensional single-bubble bulge bursting process, illustrated in Figure 5 with a 0.06-m bubble at X_t = 0.15, is very

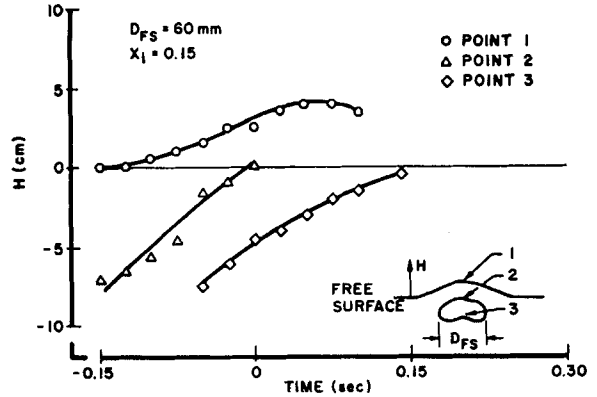

Figure 5. Trajectories of two-dimensional single bubble in 451 μm glass bed.

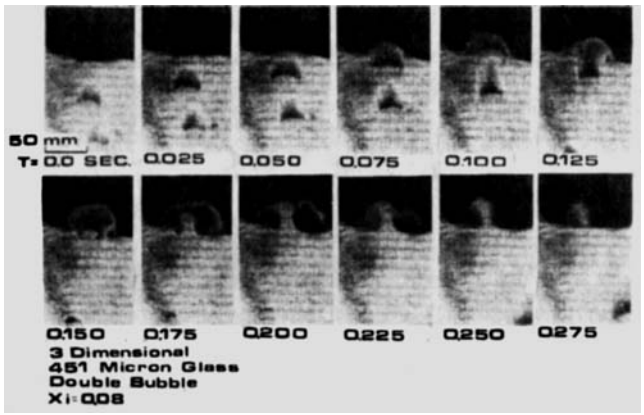

Figure 6. Three-dimensional double bubble with bulge burst, middle layer eruption and wake spike.

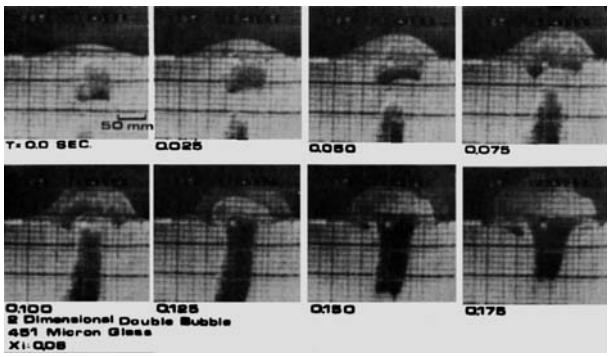

Figure 7. Two-dimensional double bubble with bulge burst and middle layer eruption.

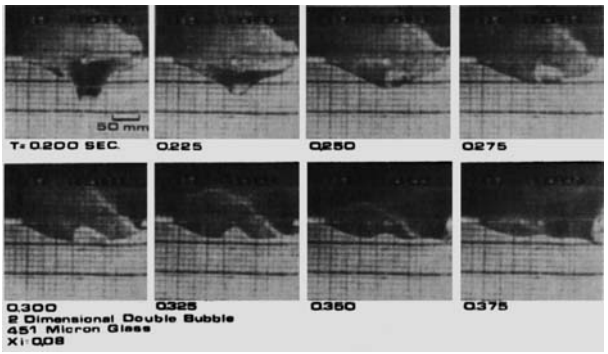

Figure 7. (continued)

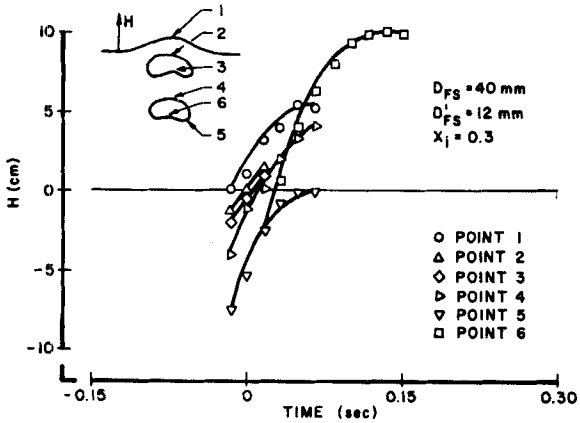

Figure 8. Trajectories of three-dimensional double bubble in 451 μm glass bed.

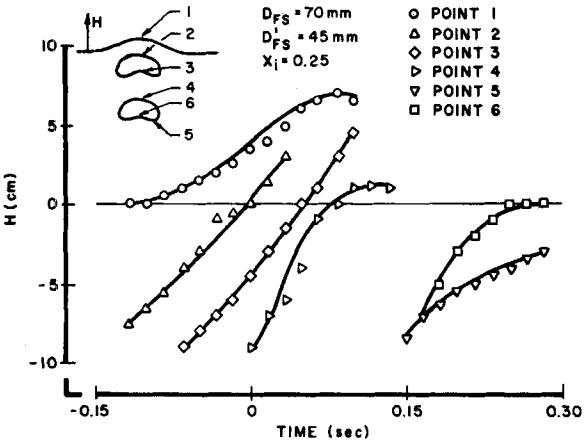

Figure 9. Trajectories of two-dimensional double bubble in 451 μm glass bed.

similar qualitatively to the three-dimensional event. The main difference between them is that the 3D wake consistently rises above the free undisturbed surface, while the 2D wake does not reach above the free undisturbed surface. In both cases, rather than splash upward, the wake remains attached to the emulsion phase like a ripple on a pool of water.

Figure 6 shows a typical eruption sequence occurring with two 3D bubbles coalescing just below the free surface. As before, this experiment was performed with 451-micron glass with approximately the same experimental conditions as shown in the previous figures. In this case, the leading bubble was 0.04 m in diameter.

The sequence of Figure 6 shows the bulge material being thrown above the bed surface at 0.05, 0.075, and 0.1 s. As a result of the coalescence of the two bubbles, the layer of solids between the bubbles (referred to here as the middle layer) combined with the leading bulge (0.100 and 0.125 s); the resulting particle cloud expanded upward and outward and then fell back to the bed surface. As the eruption process continued, the wake from the trailing bubble formed a spike which was projected above the bed surface, reaching a height in excess of the height reached by the bulge and middle layer materials. In this sequence, the initiation of the wake spike occurred at 0.15 seconds, and the spike reached its maximum height at 0.225 seconds.

Figure 7 shows a two-dimensional bubble eruption in 451-μm glass with the same test conditions which existed in Figure 6. In this case, the diameter of the leading bubble was approximately 0.07 m. This sequence shows the bulge material from the leading bubble being thrown above the bed (0.05 to 0.10 s). From 0.10 to 0.2 s, the middle layer of material was pushed into the leading bulge material forming a cloud of particles above the bed. The wake of the trailing bubble tried unsuccessfully to form a wake spike at 0.225 s. The

TABLE 3. ALL BUBBLE FREQUENCY DATA FOR EACH MATERIAL

Particle and Material	Bed	All Bubbles Which Were Double	All Double Bubbles with Significant Jet Spray	All Double Bubbles with Significant Wake Spike	No. of Bubbles Observed
125-μm Glass	2-D	8.5%	20.3%	6.8%	697
125-μm Glass	3-D	9.5%	3.4%	90.9%	1,847
756-μm Plastic	3-D	8.0%	2.5%	74.4%	1,517
112-μm Catalyst	3-D	6.9%	4.8%	85.7%	306
451-μm Glass	2-D	13.6%	4.0%	0%	845
451-μm Glass	3-D	12.9%	5.6%	73.6%	558

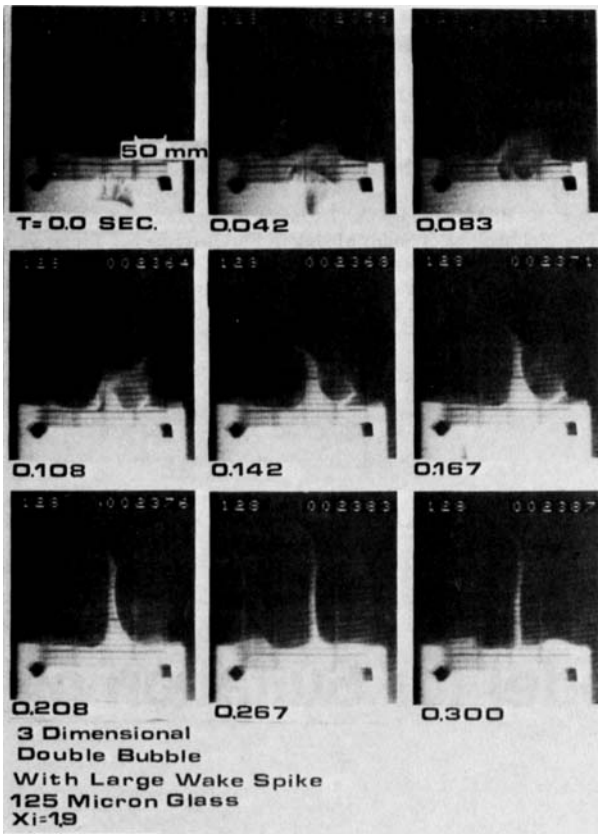

Figure 10. Three-dimensional double bubble with bulge burst, middle layer eruption and wake spike.

resulting projection of particles reached almost to the undisturbed free surface of the bed at 0.275 s, before beginning its descent.

Material trajectories for typical three-dimensional and two-dimensional bubble events are shown in Figures 8 and 9. Once again, the experimental conditions represented here are approximately the same as those shown in Figures 3 to 7. These clearly show the difference in the behavior of the wake of the trailing bubble (point 6) for the two- and three-dimensional geometries.

Analysis of a large number of bubble events showed that the wake spike phenomenon only occurred when two or more bubbles coalesced at the free surface. This phenomenon was also found to occur only in the three-dimensional bed. The strength of the wake spike phenomenon varied greatly depending on the relative positions of the two bubbles when coalescence occurred and the positions of the two bubbles relative to the free surface. If the bubbles coalesced too far below the free surface, the wake spike was relatively weak. If coalescence occurred when the bubbles were not aligned vertically, the wake spike shot off at an angle. Figure 10 shows a particularly spectacular wake spike event obtained with 125-micron glass beads in a freely bubbling bed with $X_i = 1.9$. The bubbles coalesced at 0.042 s; and the wake spike began its ascent at 0.108 s.

The fourth ejection mechanism, referred to here as the "jet spray," also was found to occur only when two or more bubbles

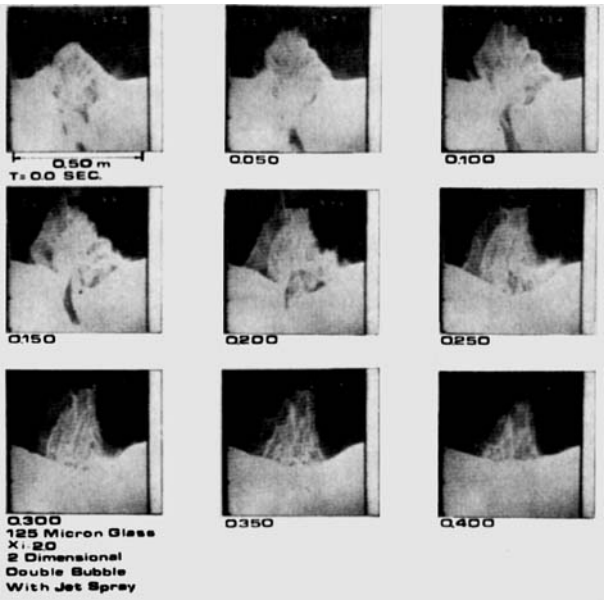

Figure 11. Jet spray mechanism.

coalesced. This is illustrated in Figure 11 which was taken with 125-micron glass at $X_i = 2.0$. The leading bubble had a 0.12-m diameter and the trailing bubble was a long, thin cavity. This provided a flow passage which allowed a jet of gas to form, entraining particles and carrying them to relatively large distances above the bed surface. The spray of particles caused by the jetting action is shown at 0.1, 0.15 and 0.2 s.

To determine the relative frequency of each of the eruption mechanisms in freely bubbly beds, all of the recorded video data was reviewed and the number of times each type of event occurred was recorded. For purposes of data reduction, only those bubbles which were greater in size than 20% of the mean bubble diameter are included in the count (i.e., if the average bubble size was 50 mm., only bubbles larger than 10 mm were counted). A single bubble is defined here as a bubble whose eruption is not affected by other bubbles. A double bubble is defined as a pair of bubbles which interact in a way which alters the eruption. Somewhat arbitrarily, the height reached by the middle layer material was used to determine if a wake spike was "strong" enough to be counted in the statistics. For example, if a wake spike occurred where the wake material did not rise as high as the middle layer, the event was not considered significant, and it was not recorded as such. The double-bubble data, Table 3, show the extreme geometry dependence of the wake spike event. Additional results, obtained to compare the behavior of beds with settled depths of 0.26, 0.52 and 1.04 m, show no apparent effect of bed depth on frequency of occurrence of any of the mechanisms.

Altogether a total of 4,228 bubbles was observed in the three-dimensional bed. Of these, 9.2% was double bubbles and 3.8% of the double bubbles showed a significant jet spray, while 72.1% of the double bubbles showed a significant wake spike. Of the 1,545 bubble events observed in the two-dimensional bed, 11.3% were double bubbles, 6.9% of the double bubbles showed significant jet spray, and 8% of the double bubbles showed significant wake

spikes. Those wake spikes which did occur in the two-dimensional bed occurred in bubbles with diameters which were of the same order as the thickness of the bed, and they were not truly two dimensional. Of the 5,773 bubbles observed, a total of 9.8% was double bubbles, and 0.47% exhibited the jet spray mechanism.

These double-bubble frequency data agree well with the results of Rowe and Partridge (1965), who reported that 11% of the bubbles observed in their three-dimensional bed was coalescing.

ACKNOWLEDGMENTS

This research is supported by the National Science Foundation under grant CPE-7926053. The authors are also grateful to Prof. Charles Smith and the Air Force Office of Scientific Research for the use of the video system which was purchased under contract F49620-78-C-0071 and to Prof. James V. D. Eppes for his assistance with the photography.

NOTATION

d_{pi} = particle diameter
$\bar{d}_p$ = mean particle diameter
D_{FS} = bubble diameter at free surface of bed
U = superficial gas velocity
U_{mf} = superficial gas velocity at minimum fluidization
X_t = $(U/U_{mf}) - 1$
ϵ_{mf} = voidage at minimum fluidization
ρ_s = particle density

LITERATURE CITED

Chen, T., and S. Saxena, "A Theory of Solids Projection from a Fluidized Bed Surface as a First Step in the Analysis of Entrainment Processes," *Fluidization*, ed. J. Davidson and D. Keairns, Cambridge University Press (1978).

Do, H., J. Grace, and R. Clift, "Particle Ejection and Entrainment from Fluidized Beds," *Powder Technology*, **6**, 195 (1972).

George, S., and J. Grace, "Entrainment of Particles from Aggregative Fluidized Beds," *AIChE Symp. Ser.*, No. 176, **74**, 67.

Horio, M., A. Taki, Y. Hsieh, and T. Muchi, "Elutriation and Particle Transport Through the Freeboard of a Gas Solid Fluidized Bed," *Fluidization*, ed., J. Grace and J. Matsen, Plenum Press (1980).

Leva, M., and C. Wen, "Elutriation," *Fluidization*, ed., J. F. Davidson and D. Harrison, Academic Press (1971).

Rowe, P. N., and B. A. Partridge, "An X-Ray Study of Bubbles in Fluidized Beds," *Transactions Institution of Chemical Engineers*, **43**, T157 (1965).

Rowe, P. N., B. A. Partridge, A. G. Cheney, G. A. Henwood, and E. Lyall, "The Mechanisms of Solids Mixing in Fluidized Beds," *Trans. Instn. Chem. Engrs.*, **43**, T271 (1965).

Zenz, F. A., and N. A. Weil, "A Theoretical-Empirical Approach to the Mechanism of Particle Entrainment from Fluidized Beds," *AIChE J.*, **4**, 472 (1958).

Manuscript received July 7, 1981, revision received March 2, and accepted April 30, 1982.

Distributed Pore-Size Model for Sulfation of Limestone

A model is proposed to study the reaction between a porous solid and a reactant gas resulting in solid and gaseous products. The model describes the reacting solid as a sphere made up of a distribution of randomly oriented open pores. The evolution of the pore-size distribution is followed by use of a population balance, using a combination of the independent variables of time and location first presented by Dudukovic (1976). The macroscopic properties of the solid are obtained by integrating over the pore size distribution. The results of the population balance are used with a mass balance on the reacting gas to obtain rate and conversion data.

The results of the model are compared to experimental data obtained for the sulfation of limestone (Ulerich et al., 1977). Both rate vs. conversion as well as conversion vs. time plots are presented, which serve as a more strenuous test of the model than either type of plot alone.

P. G. CHRISTMAN
Department of Chemical and Nuclear Engineering
University of California
Santa Barbara, CA 93106

T. F. EDGAR
Department of Chemical Engineering
The University of Texas at Austin
Austin, TX 78712

SCOPE

The distributed pore model is the first attempt to characterize the solid structure, in a gas/solid reaction undergoing pore closure, with a distribution of pore sizes instead of an average grain or pore size. This model accounts for four resistances to the overall reaction. These resistances include mass transfer across a mass transfer boundary layer, through the porous medium and through the solid product as well as surface reaction kinetics. The relative importance of the resistances depends on both the initial pore size and the extent of conversion. One feature of most previous models based on an average pore or grain size was a sudden cut off of the reaction at the point of pore closure. The experimental data do not show this type of behavior but the rate tends to gradually decrease as the outer layer is plugged. Hartman and Coughlin (1976) overcame this problem with their grain model by noting that a certain amount